Implementing an AI That Automatically Extracts Standardized Functional Patterns From Wearable Sensor Data

Implementing an AI that automatically extracts standardised functional patterns from wearable sensor data

Vini Vijayan, James Connolly, Joan Condell, Nigel McKelvey, and Philip Gardiner

***Abstract*— Standardised functional tests (SFTs) are frequently used to quantify a person's ability to perform activities of daily living against expected values. SFTs provide valuable information to aid a clinician's understanding of a patient's status and direction of improvement. Such information may support clinicians when assessing a wide range of conditions such as musculoskeletal or neurological diseases or age-related frailty. If these SFTs could be performed reliably by patients in their own home without supervision they could track and help to guide rehabilitation. Wearable devices have the potential to collect reliable data from the wearer when performing SFTs. However, the data generated from sensors for long-term recordings of movement can become very large, making it difficult to manually extract movement information with any level of accuracy. Hence, it is important to evaluate whether it is possible to implement an automated system capable of extracting SFT patterns from long-term sensor data without manual data processing.**

This paper describes an Artificial Neural Network system that was trained to extract specific SFTs such as the 30-second Chair Stand Test (30s-CST) and the 40-meter Fast-Paced Walk Test (40m-FPWT). The resultant model obtained 99.7% accuracy in 30s-CST pattern recognition, 99.3% accuracy in 40m-FPWT pattern recognition, and 97.3% accuracy in detecting false patterns. The system provided an overall accuracy of 98.76% with supervised clinical trial data. The ambulatory data testing phase obtained an overall accuracy of 90.18%. Specifically, it achieved 92.73% accuracy in detecting 30s-CST patterns and 86.67% accuracy in recognising 40m-FPWT patterns.

***Index Terms*— Wearable technology, Activities of Daily Living (ADL), Artificial Intelligence (AI), Artificial Neural Network (ANN), Standardised Functional Test (SFT).**

I. Introduction

The functional status of a person can be quantified by their ability to complete functional assessments, commonly known as standardised functional tests (SFTs) [1]. These are often utilised to compare a person's functionality to standardised expected values [2], and assess the quality of a person's health status. SFTs are used to assess a person's functional ability within a clinical setting, rehabilitation assessment, age-related movement difficulties, and various musculoskeletal disorders [3][4]. Some clinicians advocate their use as a reliable measure of functional performance to assess weight transfer between legs, gait and turning movements [5]. It is widely recognised that performance in these tests is strongly linked to functional ability and independent living [6], [7]. Furthermore, SFTs provide valuable information to aid a clinician's understanding of a patient's current disease status and direction of improvement [8], [9]. Common SFTs include the 30-second sit-to-stand test , also known as the 30-second chair stand test (30S-CST) [10], the "timed Up & Go" test (TUG), the six-minute walk test (6MWT), and the 40 meter walk test (40MWT) [7]. Patients can be assessed on their ability to complete specific SFTs that are relevant for the disease under scrutiny. For example, the 6MWT is commonly used for the objective assessment of functional exercise capacity in the management of moderate-to-severe pulmonary disease and the coexisting extrapulmonary manifestations of chronic respiratory disease, including cardiovascular disease, frailty, sarcopenia, and cancer [11]. The TUG test is used to measure gait speed, and is a reliable outcome measure for various musculoskeletal or neurological diseases [12]. Research studies using SFTs are becoming commonplace, and most are investigated within a controlled clinical environment, under expert supervision.

An inertial measurement unit sensor (IMUs) is an electronic device that detects object movement, angular rate, and direction. An accelerometer, gyroscope, and magnetometer work together to achieve this. One or more accelerometers can identify linear acceleration, gyroscopes can detect rotational rate, and the magnetometer readings can serve as a heading reference [13]. IMUs are commonly implemented within wearable devices to provide continuous monitoring of the wearer. Such devices can be used for clinical assessment when

Vini Vijayan is with the Computing Department, Atlantic Technological University (ATU), Letterkenny,F92FC93,Ireland; (e-mail: vini.vijayan@atu.ie)
James Connolly is with School of Computing, Engineering & Intelligent System, Ulster University, Magee Campus, Londonderry, BT48 7JL, Northern Ireland (e-mail: jp.connolly@ulster.ac.uk)
Joan Condell is with School of Computing, Engineering & Intelligent System, Ulster University, Magee Campus, Londonderry, BT48 7JL, Northern Ireland (e-mail: j.condell@ulster.ac.uk)
Philip Gardiner was with the Rheumatology Department, Altnagelvin Hospital, Glenshane Road, Londonderry, Northern Ireland; (e-mail: pvgardiner@gmail.com)
Nigel McKelvey is with the Computing Department, Atlantic Technological University (ATU), Letterkenny, F92FC93,Ireland; (e-mail: nigel.mckelvey@atu.ie)

placed on specific locations of the patient's body, such as the wrist, neck, back or waist [14]. Previous research has proven that IMUs demonstrate encouraging results as a low-cost method of quantifying human movement [15]–[20].

Studies have examined the effectiveness of IMU sensors as a data collection method for SFTs. Greene et al [21] used leg worn wearable sensors to collect data corresponding to the 5-repetition chair stand test (CST) for estimating balance, cognitive function, and participant risk of falling. 168 elderly individuals completed the Mini-Mental State Examination (MMSE) and the Berg Balance Scale (BBS) tests. The MMSE and BBS are standardised paper-based assessments that measure cognitive function and functional balance, respectively. The maximum achievable score for the MMSE is 30, with values of 25 or higher considered normal. Clinicians often view scores under 24 as abnormal, indicating potential cognitive impairment. The BBS is a five-point scale that ranges from 0 to 4. "0" represents the lowest level of function, and "4" represents the highest level of function [22], [23]. Each participant performed five repetitions of the CST with IMU sensors placed on both the thigh and torso. The test was conducted either in a home or in a clinical environment. Each sensor was used to extract features that measured time duration, postural instability, and variability of the test. The study researchers implemented the Spearman's nonparametric correlation test to examine the relationship between MMSE and BBS features [24]. Their findings demonstrated cross-validated classification accuracies for balance impairment, cognitive decline, and falls risk were 81.96, 72.71, and 68.74%, respectively.

Martinez-Hernandez et al [25] presented an approach that detected sit-to-stand (SiSt) and stand-to-sit (StSi) activities, utilising a Bayesian formulation and a sequential analysis method utilising IMU sensors attached to the thigh of participants. Despite the presence of sensor noise, this system implemented algorithms that could automatically analyse sensor data during the data collection phase. Their probabilistic technique accurately detected the activity stages of sitting, transitioning, and standing by analysing supervised data from a wearable IMU sensor. The results obtained in an offline mode showed a recognition accuracy of 100% for all activity levels and phases, with an average reaction time of 50 ms to make a decision about activity state and transition phase.

Psaltos et al [26] assessed leg muscle function using IMU sensors to record movement whilst performing the Stair Climb Power Test (SCPT). They proposed an algorithm to classify stair climbing periods and estimate stair climb power from a lower-back worn accelerometer. Data were collected under laboratory conditions from 65 healthy adults who performed the four-step SCPT and a walking assessment. Using two classifiers distinguishing stair ascending from stair descending and stair walking from level walking, and ensemble machine learning (ML) algorithms trained on accelerometer signal features, the system was able to identify periods of stair ascent with >89% accuracy (sensitivity = >0.89, specificity = >0.90). The model's performance showed minimal differences when using only the gyroscope (±0–6% accuracy) compared to the accelerometer model, although there was a small improvement in accuracy when the gyroscope and accelerometer were combined (approximately +3–6% accuracy).

Cobo et al [27] presented a system comprised an IMU sensor on the subject's thigh that detected and counted SiSt transitions in real-time. Under supervised conditions, automated sensor counts exhibited a strong correlation with the researcher's manual counts. The paper analysed the system's compatibility with the abilities and expectations of older individuals, allowing them to use it independently at home without supervision. This approach did not address the challenge of automatic detection of SFTs. However, researchers conducted this study to determine if the system could meet the needs and expectations of older individuals, enabling them to use sensors independently.

The data acquired by sensors in clinical settings such as those described above, are relatively small in file size and therefore straightforward to manipulate and analyse. However, in an ambulatory setting, the data collected by IMU sensors can become enormous in tuple size, making it laborious, prone to error, and time consuming to manually extract SFT patterns from such datasets. As a result, despite their validation as a measurement of functional ability, to date SFTs have not been widely used for movement evaluation in home settings. The aim of this paper is to describe the techniques needed to design and develop an AI system that can automatically extract SFT patterns such as the 30S-CST and the 40m-FPWT from data collected using DorsaVi's ViMove system [28] when used in an unsupervised ambulatory environment [29]. ViMove is a Food and Drug Administration (FDA) approved wearable technology system with integrated IMU sensors that accurately measures, records, and reports lower back / lumbar spine movements and muscular activity. The wireless ViMove sensors used in this study have high reliability in monitoring spinal movements [30]. However, even with this system the extraction of SFT's can be technically challenging, and prone to movement misclassification. To the best of our knowledge, the methods described in this work have not been implemented by any commercial wearable monitoring systems.

II. MATERIALS AND METHODS

The objective of this research was to examine the efficiency of an AI system in detecting and extracting SFT patterns from a large dataset over a long period of time. This research study consisted of 30 participants recruited from the student and staff population in the Atlantic Technological University (ATU), Donegal Campus, Ireland. All subjects gave their informed consent for inclusion before they participated in the study. The study protocol was approved by the Ethics Committee of the Atlantic Technological University (ATU),

Donegal Campus, Ireland. In this study, each participant was monitored under supervised and unsupervised sessions. Movement data was recorded throughout each session using the ViMove system [31].

Inclusion Criteria set for this research study were:

- Participants were aged between 18 – 55
- Participant body mass index (BMI) was between 18.5 – 24.9 (normal BMI range)

Exclusion Criteria were:

- Severe joint or spinal pain at the time of the study
- Severely restricted hip movement
- History of previous vertebral fracture
- History of previous spinal surgery, scoliosis deformity
- Pregnancy

This research was carried out in two sessions. The first "supervised" session was completed in a controlled environment. A study researcher guided and advised each participant throughout completion of each SFT exercise. The Recording and Feedback Device (RFD) shown in Fig. 1(b) is an essential component of the ViMove system, and it is approximately the same size and weight of a small mobile phone. The RFD wirelessly received data collected from each of the ViMove IMU sensors and stored this data for offline download once each session ended.

Fig. 1. (a) Sensor positioning using a fitting template, (b) RFD device for ViMove IMU sensors.

In this study, the RFD stored data corresponding to wearer movements, which were then subsequently extracted from the device by connecting it to a laptop using the proprietary ViMove application. The RFD device also had a MODE button for switching between data collection modes. The MODE of operation was set to "supervised" for supervised data collection, and "monitoring" for ambulatory data collection. To collect supervised data, the RFD device was connected to the IMU sensors, and then configured for either "supervised" or "monitoring", depending on the mode of data collection. The datasets in the supervised mode, which are live assessment data, are smaller in size than those in the monitoring mode.

IMU sensors were attached to the participant's body using a positioning template shown in Fig.1(a). The lower sensor was located between the superior iliac spines, and the upper lumbar (trunk) sensor was positioned above the T12 vertebra. In this study, sensor placement and body postures during SFT movements were important factors, as variations in either may affect the structure of the SFT pattern. During ambulatory monitoring, we allowed the participants to engage in their usual activities, like walking, running, or visiting a gym. However, no positional displacement of the sensors was observed during the data collection.

The RFD permitted users to indicate the start and end of SFT movements by pressing the 'EVENT' button. When the EVENT button is pressed, the ViMove system adds a marker in the IMU data. This marker helps identify the beginning and end of movements. This is a common approach that is used in clinical trials that employ IMU sensors for SFT detection. However, this method can potentially introduce a time delay between the user's initiation of the start button and movement commencement. If the EVENT button is pressed a few seconds before starting an exercise, unrelated sensor data gets added to the movement pattern. This extra data affects the accuracy of the patterns used for classifier training. Due to these concerns, in this study, we did not manually record the start and end of each movement using the EVENT button. As a result, the data gathered during the supervised session were small in size but unlabeled. We analysed the structure of these movement patterns in detail in a previous clinical study [32] and then used these feature values to design an algorithm to extract SFT patterns from the supervised dataset. This algorithm can be used by any supervised monitoring environment to extract 30s-CST and 40m-FPWT patterns. We can also avoid implementing a manual method to indicate the start and end positions of movement within recorded data.

A. Supervised and unsupervised ambulatory monitoring

Data captured using wearable sensors during a supervised monitoring session is typically gathered within a short time period, depending on the type and number of recorded exercises under measurement. A common disadvantage of supervised monitoring is that patients typically visit a clinic or research lab for data collection, and the data collection process is completed by an expert who is knowledgeable in the setup and control of the wearable device, as well as sensor data extraction methods.

A study participant may be more focused and aware of their gestures and motions when under close scrutiny and will concentrate on the correct completion of exercises. Since participants do not typically move with such focus, then it is quite common for supervised recorded movement to differ significantly from a participant's "free-living" movement patterns. Therefore, it is important to capture recommended exercises from participants such as SFTs when at home. Hence, participants were instructed to complete the same set of SFTs three times at home, with breaks in between, at their leisure. The second "unsupervised" phase of the study was therefore completed in the participants home environment without researcher guidance. Before starting ambulatory monitoring, the participants were provided with both video

and written instructions on how to perform the tests at home. Each participant completed a diary to record the approximate time they completed each SFT, and the number of repetitions within each one. And they recorded if they encountered difficulty during each test, or if they stopped a test without finishing. This diary was used to compare the system output with expected SFTs.

B. 30-Second- Chair Stand Test

During the study, participants performed two SFTs: the 30-second Sit-to-Stand Test (30s-SCST) and the 40-meter Fast-paced Walk Test (40m-FPWT). These tests were initially conducted in both a supervised and unsupervised monitoring setting. Subsequently, the tests were conducted in a long duration ambulatory setting. The 30s-CST activity determines the maximum number of chair sit-to-stand repetitions possible within a 30 second period. The initial objective of 30s-CST was to evaluate leg strength and endurance in elderly people. This test was designed to address the floor effect of the five- or ten-repetition sit-to-stand test in older people. 30s-CST is also being considered as a physical performance test for young adults and athletes, although further research is needed [33].

During the 30s-CST, each participant sat on a chair in a position that allowed them to place their feet flat on the floor, shoulder width apart, with knees flexed slightly more than 90 degrees. The arms were crossed at the wrists and held across the chest. Each participant stood up completely from the sitting position, allowing the hips and knees to fully stretch, then returned to the sitting position, allowing the bottom to fully touch the seat. This movement was repeated for 30 seconds.

C. 40 Meter Fast Paced Walk Test

A 40m-FPWT is a 40-meter walking activity that assesses a participant's short-distance walking speed and their ability to change direction while walking. This test is important because a combined exercise of walking and turning is the most effective method for detecting balance issues in an individual. It is often not possible to use this assessment in elderly people and those with restricted hip and/or knee movement. During the 40m-FPWT, participants walk as quickly but as safely as possible along a 5-meter walkway without running, then turn around a cone, return, and repeat for a total distance of 40 meters [34]. The measurement criterion for 40m-FPWT is quantified as the total time required by the participant to complete the test. When designing the 40m-FPWT pathway, it is important to ensure that participants have sufficient room to turn around at each cone, and there should be a clear signpost indicating the starting point of the test. During supervised monitoring, the researcher can initiate each repetition when the participant reaches this position, ensuring that all movements are recorded with consistent data points for further analysis.

D. Standardised Functional test Patterns for 30s-CST and 40m-FPWT

Fig. 2 shows typical patterns for the 30s-CST and 40m-FPWT. When the accelerometer and gyro meter readings are combined, a single sit-to-stand movement contains two peak values: the first reflects the flexion of the upper body as it begins to move from the chair, and the second depicts the completed standing posture.

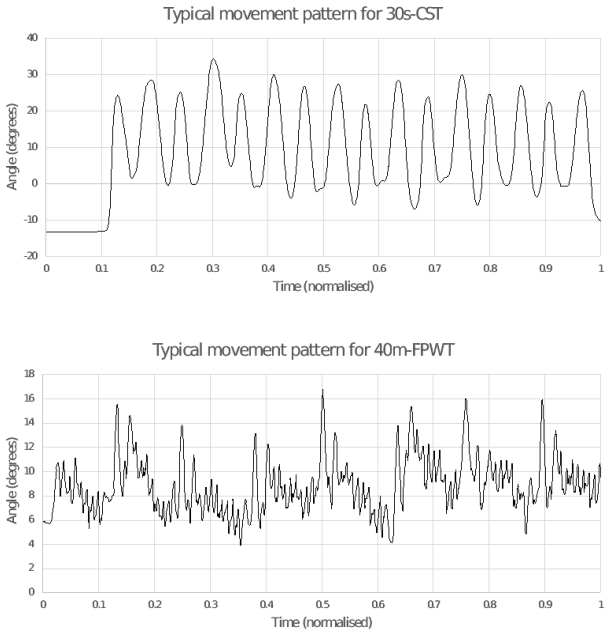

Fig. 2. Typical movement pattern for 30s-CST and 40m-FPWT

The angular value then decreases to a sitting posture. Hence, the number of peaks in the 30s-CST pattern is twice that of a typical sit-to-stand movement. The 40m-FPWT pattern consists of walking and a turn. The walkway in this study was configured at 5 meters. As a result, 7 turnings were required in the 40m-FPWT. The ViMove sensors used in this study were attached to the participant's upper body. While walking, the upper torso exhibits less mobility compared to the legs. Hence, the recorded data did not accurately represent the changes in angular values with respect to the number of steps taken. So, during data analysis, if a matching pattern existed, and the number of turnings were more than 7, then the first eight patterns were analysed. And if the number of turns were less than seven, then the movement was not considered as an SFT for the purpose of this study.

Each SFT movement pattern is complex in structure, and each repetition within the same SFT may exhibit individual pattern structures due to minor variations in body gestures and movement speed. Training and testing an AI system to recognise long, structurally diverse patterns pose significant challenges. To improve system accuracy, each SFT pattern was segmented into individual movements (feature extraction) and then processed accordingly.

III. Artificial Neural Network System Design

This study did not manually record the start and end of any movements. Instead, we designed an algorithm to extract specific SFT patterns through pattern recognition using feature values. Initially, we used the system to extract each SFT pattern from a short-duration unsupervised data set. We then used the retrieved patterns to train the ANN system.

A. Data preprocessing

The ViMove IMU sensors output data that contains accelerometer, gyrometer, and magnetometer values. First, we converted the accelerometer and gyrometer readings' x, y, and z coordinates to quaternions. Quaternions are a four-dimensional numerical system in mathematics that may represent rotations and orientations[35]. After combining the accelerometer and gyrometer values, we calculate their orientation and rotation during movement using composite quaternion operations. Using the quaternion rotation method, we combined the previous positional coordinate data with the corresponding quaternion vector to generate the final positional coordinate for each object. Our previous work [36] provides a detailed explanation of the data preprocessing steps.

B. Feature Extraction

Examining each SFT pattern in detail uncovers unique movement patterns that can help to characterise and recognise features of each SFT. For example, when analysing sensor data collected from the 30s-CST, it was evident that each movement pattern structure began at a lower angle which gradually incremented to a maximum angle.

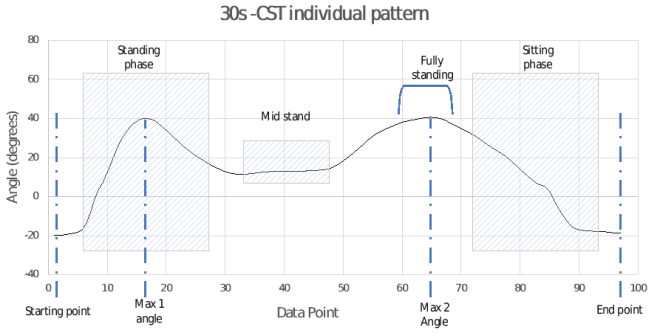

Fig. 3. Individual movement pattern for 30s-CST.

The movement pattern then dipped before returning to the second maximum angle, and then decreased to the minimum angle, which represented the stopping angle for this specific SFT. There were two maximum values for individual sit to stand movements. Fig. 3 depicts the minimum, maximum and mid-stand points for an individual movement pattern for the 30s-CST.

TABLE 1. FEATURE VALUE OF 30S–CST MOVEMENTS.

Start angle [1]	Max1 angle [2]	Max2 angle [3]	Stop angle [4]	Average time duration between max1 and max2	Time duration (Total seconds)	Repetition (seconds)
<0*	5<=max1 <=70*	5<=max2<=70 *	<10*	1 sec to 4.5sec	2 sec to 6 sec	>=5 and <=15

1 Start angular value for a 30s-CST movement pattern.
2 Maximum angular value for the first peak in the 30s-CST movement pattern.
3 Maximum angular value for the second peak in the 30s-CST movement pattern.
4 Stop angular value for a 30s-CST movement pattern.
*Angular value in degrees

Each study participant typically required between 2 and 6 seconds to complete one CST movement. One SFT participant session contained 5 to 15 repetitions of the 30s-CST patterns, with an average of 12 repetitions per participant. Table 1 shows the feature values created for the 30s–CST.

In the 40m-FPWT, each repeating movement has a distinct pattern structure, as well as varying completion times, and a distinct average number of steps. We examined multiple 40m-FPWT patterns to determine the feature values, and we entered the angular values for the minimum and maximum angles in a relaxed manner to ensure we didn't overlook any patterns during processing. Table 2 shows the feature values that were used to extract the 40m-FPWT patterns in this study.

TABLE 2. FEATURE VALUE OF 40M-FPWT PATTERNS

Minimum angle [1]	Peak angle [2]	Step Count [3]	Time duration	Repetitions
>= -30*	<=35 *	>= 5 and <=15	5 sec to 11sec	8

1 Minimum angular value for a 40m-FPWT movement pattern.
2 Maximum angular value for a 40m-FPWT movement pattern
3 Number of steps taken to complete a 40m-FPWT movement.
* Angular value in degrees

The participant's turning point is visually recognisable as a peak within the movement pattern, and is therefore used to denote a physical turn within the SFT [37].

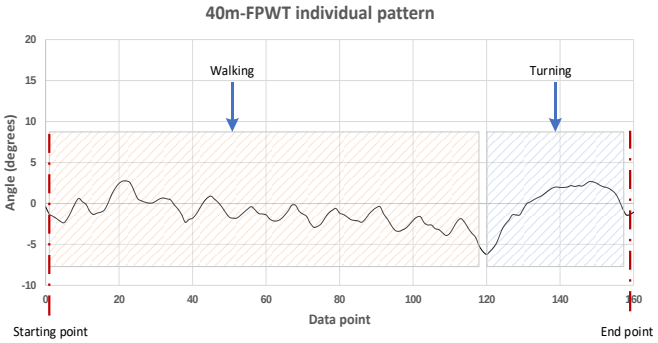

Fig. 4. 40m-FPWT Individual Pattern

Therefore, counting the number of peaks within the segmented data represents the number of turns within the SFT. Fig. 4 shows a pattern for a typical 40m-FPWT.

C. Data Segmentation/Movement Extraction Algorithm

Following the definition of feature values for the 30s-CST and 40m-FPWT, each sensor output was analysed for patterns that matched the specific feature values. The algorithm for segmenting input datasets using feature values was divided into two phases. The first phase identified various movement patterns, and the second phase extracted patterns that matched the current feature values. We constructed this module to trace each SFT pattern according to their unique shape, mapping the angular values to 0 or 1 depending on their direction of change (increasing/decreasing). Our previous paper outlined the data segmentation process with pseudocode [32]. The extracted matching patterns were compared to the feature values. If the movement matched to all the features, it was transferred to a

new dataset that contained motions that matched to each of the feature values.

D. Similar Pattern generation

There were 30 participants involved in this study session. We extracted 319 patterns matching to 30s-CST, and 240 patterns matching to 40m-FPWT from the supervised clinical trial. However, in comparison to the complexity of the ambulatory data, the number of extracted patterns for training the AI system was quite small. Therefore, we utilized statistical methods to extract the minimum, maximum, mean, and median values from each SFT dataset. We then utilized this information to create additional synthetic data using mathematical functions like sum, difference, multiplication, division, and exponent. We combined similar patterns from the existing dataset to create more movement patterns that matched the 30s-CST and 40m-FPWT sensor data.

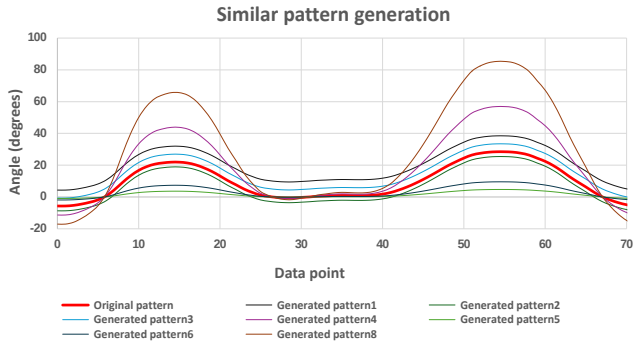

Fig. 5. Similar patterns generated from the original pattern for a 30s-CST movement.

Fig. 5 shows an example of similar patterns generated from the original pattern for a 30s-CST movement. The figure presents multiple examples of synthetic data, demonstrating that there are multiple additional patterns necessary to encompass all combinations of minimum and maximum movement not represented in the original dataset. Patterns 2, 5, and 6 exhibit angular values that are lower than those of the original pattern (highlighted in red), while all other patterns show higher values compared to the corresponding angular values of the original pattern. The generated patterns should have structures comparable to 30s-CST or 40m-FPWT patterns. The new synthetic patterns were compared to the original SFT from which they were generated to ensure pattern consistency.

E. Data Padding

The number of data points in each movement pattern is determined by the sensor sample rate (Hz), and the time taken by the participant to complete each movement. The number of data points may differ between participants and for each SFT. However, the ANN system required the same number of data points for all patterns in the training and testing phase [38]. Therefore, when generating a training dataset for ANN, one of our bespoke algorithms checked the maximum number of data points in the entire existing dataset. If the newly generated pattern had more data points than the existing patterns, it modified all other patterns by padding the current pattern's start and end values to extend their data points without changing their original shape. If not, it updated the current pattern to align with the data set.

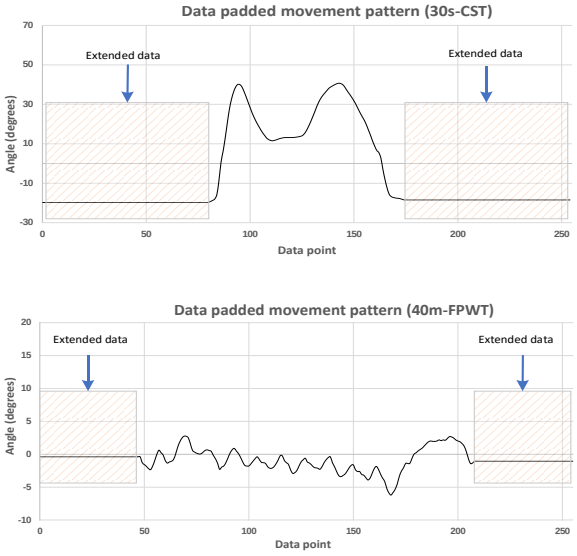

Fig. 6. 30s-SCT and 40m-FPWT patterns after data padding

Fig. 6 depicts the shapes of 30s-SCT and 40m-FPWT patterns after data padding.

F. False Movement pattern Generation

After processing the entire supervised clinical trial dataset for movement extraction, more synthetic data patterns were generated using the python random.uniform() function to include non-SFT patterns into the training dataset. This step was important during the AI system design process; otherwise, the ANN system could become confused by random movement patterns that do not match any SFT patterns.

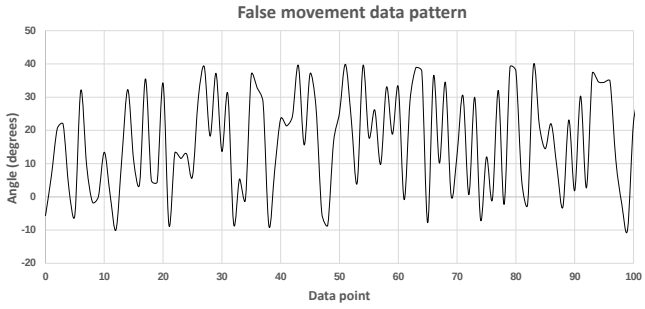

Fig. 7. Random movement data pattern

We trained the ANN system using the random movement patterns generated in this step, which included all other movements except SFTs with a distinct output. To train the ANN system, the number of points in the false movement pattern should match the number of data points in the SFT patterns. During the initial phase, we included an equal number of false movement patterns as those used for SFT. Hence, the ANN system required a considerable amount of time to process the complete dataset. To optimise space usage and enhance processing efficiency, we eliminated false movement patterns step-by-step while maintaining system accuracy. Consequently, we reduced the number of false movement patterns to 25% of the total dataset. Fig. 7 depicts some random movement patterns generated by the system.

After generating each pattern in this phase, the system checked the variance of that pattern to ensure that it was significantly less or significantly higher than the variance of actual SFT patterns.

G. Labelling the Extracted patterns

The extracted movement patterns for 30s-CST and 40m-FPWT, as well as the random patterns, were labelled separately. The 30s-CST patterns were labelled as 0, the 40m-FPWT patterns as 1, and the random movement/unrecognized SFT patterns as 2. Hence, the unsupervised dataset was converted to supervised data, and was then ready for use in training the ANN system.

H. ANN system design

Neural networks can rapidly acquire features and demonstrate greater adaptability compared to traditional network classifiers in executing data classification tasks. Recent research activities indicated that the neural network classifier is a promising alternative to traditional classification techniques, as it possesses the ability to learn independently and generate outputs [39]–[41]. In this research, we experimented with classification using multi-label decision trees and random forests. However, due to the high volume of data and the complexity of the pattern structure, the accuracy during the testing phase was significantly low. The training and testing phase utilised a 70:30 data split; the multi-label decision tree showed an overall accuracy of 36.4%, while the random forest had an accuracy of 42.7% in classifying 30s-CST and 40m-FPWT. ANN are characterised by their ability to learn complex nonlinear correlations between inputs and outputs, utilise sequential training techniques, and adapt efficiently to data. The predominant family of neural networks utilised for pattern classification problems is the feed-forward network, encompassing the multilayer perceptron [42].

The ANN system training phase used a 70:30 training/testing split. The ANN system was presented with 27817 patterns of 30s-CST and 24456 patterns of 40m-FPWT, and 17352 synthetic data patterns, totalling 69625 patterns. The ANN system was designed using Keras and TensorFlow [43], with 256 nodes in the input layer, 16 hidden layers with 64 neurons, and 3 neurons in the output layer. The input layer consists of the maximum number of data points currently identified in the 30s-SCST or 40m-FPWT movement patterns. In the output layer, '0' represented the 30s-CST, '1' represents the 40m FPWT, and '2' represents all data patterns other than 30s-CST and 40m-FPWT.

I. ANN training and testing

During the training phase, the ANN system was trained with a large number of variants of labelled 30s-CST and 40m-FPWT SFT patterns. The ANN testing module was combined with the data segmentation/ movement extraction phase to eliminate the need for additional storage of intermediate patterns. Each new pattern extracted was simultaneously passed to the ANN testing phase. If the new input pattern had similar structure to the 30s-CST patterns in the trained data, the ANN system returned '0,' for the 40m-FPWT the system returned '1,' and for all other data the value '2' was returned. Patterns with '0' and '1' values were extracted and separated for subsequent processing. AI system testing generated a large output file since it contained all individual patterns that corresponded to sit-stand and walk-turn activities. However, not all of them were SFT patterns.

J. Hierarchical Clustering

The next stage in the AI testing process was hierarchical clustering of data points from the dataset obtained after the ANN system testing phase. The dataset contained all the data points (individual movements) that corresponded to the shape and feature values of the corresponding SFTs. As previously stated, all of these movements were not included in SFT. This hierarchical clustering module was programmed to extract the actual SFT patterns from the matching pattern dataset obtained from the ANN system.

The hierarchical clustering module had a layered structure. The bottom layer read all of the output patterns from the ANN system. Each top layer was programmed to merge movements from its bottom layer with respect to the specified window length. In this system, the window length was fixed to the time duration. Hence, the hierarchical clustering phase merged movements that were close together or occur within a specific time period. We set the duration of the 30s-CST window for first-level processing to a maximum of 40 seconds. When two movements occurred within a continuous 40-second time span, we combined and pushed both clusters to the next-level cluster. Then, for the subsequent layers, we merged two clusters with N and M elements, or N>M, if (M-2) elements occurred within the window length of N-elements in the first cluster. All clusters with at least four elements are considered for the next stage of processing. We set the distance metric for 40m-FPWT pattern recognition at 50 seconds. Clusters containing at least 8 components (40m-FPWT expecting 8 repetitions of the individual pattern) were eligible for next-level processing. 30s-CST and 40m-FPWT had different time durations and were returned to different files from the ANN system. This phase can be accelerated by running them parallelly.

IV. Results

The ANN system was ready to recognise SFT patterns once training and testing were completed. However, the real time ambulatory data was too large, complex, and unseen in comparison to the clinical trial data. Therefore, we modified the AI system so that it could recognise SFT patterns accurately. AI system testing for unseen data was conducted in two phases. In the first phase, 5 participants wore the ViMove system in a supervised clinical session. Once this session ended, participants performed SFTs using the ViMove system without supervision. Each participant repeated each SFT twice. Then each participant wore the ViMove system at home, repeated each SFT at three random times and recorded the data in their diary.

The data preprocessing steps for system testing were similar to those for the training phase. The data segmentation algorithm implemented for the supervised data set worked well for

extracting patterns during the first phase of unsupervised data collection. We modified the data segmentation/movement extraction algorithm for long-term ambulatory data by dividing the entire dataset into chunks of 50000 data points. We took this action because the data subset included approximately 20 minutes of data, which is the maximum duration required to complete 30s-CST and 40m-FPWT consecutively. It is not recommended to split the SFTs between two consecutive chunks, as this could lead to a loss of pattern identification and a decrease in overall system accuracy. To prevent that, we included the maximum number of data points each SFT could have at the start and end of the data set from the preceding and subsequent subsets. We then processed these chunks simultaneously to minimise execution time. We implemented this by running multiple processes in parallel using the ProcessPoolExecutor() function in Python and extended the feature window to guarantee the extraction of every SFT pattern. The system automatically expanded the existing dataset to align with the processing capabilities of the ANN for pattern matching if it recognised a pattern with a larger number of data points. We analysed different combinations of epochs and batch sizes, adjusting the epoch from 20 to 200 and the batch size from 200 to 2048, depending on the dataset size. We set the 'epoch' to 50 and the batch size to be 1024 after analysing the learning curve for accuracy and execution time of the model.

Activation functions introduce nonlinearity, enabling neural networks to learn complex patterns and make predictions [44]. After analysing the model's learning curve, the activation function 'tanh' was used for all levels except the output layer. The tanh activation function yields outputs that range from -1 to 1. It is beneficial for data that exhibits both positive and negative output characteristics, and it facilitates faster model training, which is an essential consideration when addressing complex models and large datasets [45]. The output layer had a 'softmax' activation function. In multi-class classification tasks, the Softmax activation function transforms raw, unbounded values into a probability distribution across multiple classes.[46]. In this study, in the output layer, '0' represented the 30s-CST, '1' represented the 40m-FPWT, and '2' represented all data patterns other than 30s-CST and 40m-FPWT.

TABLE 3. CONFUSION MATRIX FOR THE ANN SYSTEM

Confusion Matrix	30s-CST	40m-FPWT	Other Patterns
30s-CST	11735	3	31
40m-FPWT	12	6107	27
Other Patterns	46	33	3023

The ANN system split the data set into training and testing datasets. It took 48738 patterns to train and 20887 patterns to test the system. The system had a loss value of 0.0657 and an overall accuracy of 98.6%. The confusion matrix in Table 3 is interpreted as follows: 11735 of 11769, 30s-CST patterns were correctly identified, while 3 patterns were classified as 40m-FPWT and 31 were classified as other patterns. From 6146 40m-FPWT patterns, 6107 were correctly recognized, while 12 were classified as 40m- FPWT and 27 were classified as other patterns. 3023 of the 3102 fake patterns were identified as false patterns, while 46 were classified as 30s-CST and 33 were classified as 40m-FPWT.

We also analysed the pattern structure of individuals who had the same height, weight, and BMI, considering their gender classification. However, we found no significant correlation between pattern structures in this context.

A. System Testing output for unseen data

The AI system testing phase included ambulatory data from five participants.

TABLE 4. SUMMARY OF SFTS FROM PARTICIPANT'S DIARY

Participant ID	30s-CST			40m-FPWT		
	1st round	2nd round	3rd round	1st round	2nd round	3rd round
FOR01A1	14	12	12	8	8	8
FOR02A1	6	8	8	8	8	8
FOR03A1	12	11	12	8	8	8
FOR04A1	11	10	12	8	8	8
FOR05A1	13	12	12	8	8	8
Total	165			120		

According to the participants' diaries, they performed in total 165 of 30s-CST movements, 120 of 40m-FPWT movements throughout three rounds of SFT repetition at home. Hence, the ambulatory dataset consisted of 285 SFT patterns from 5 participants. Table 4 shows a detailed summary of each participant's movements. The AI system testing module was then provided with the ambulatory data set.

TABLE 5. CONFUSION MATRIX

SFTs	30s-CST	40m-FPWT	Normal movement
30s-CST	153	0	12
40m-FPWT	0	104	16

After examining the output of the AI system and reviewing the participant's diary, it was found that the system correctly identified 153 out of 165 30s-CST movements. However, it was unable to identify 12 movements. Out of the 120 40m-FPWT patterns, 104 were correctly recognised, while 16 movements went undetected. During the ambulatory monitoring, some participants failed to complete the 30s-CST, and some missed the count when performing the 40m-FPT. Additionally, some participants turned in the 40m- FPWT was incorrect, making it challenging to identify these patterns. All these factors might be affected accuracy the ANN system.

The confusion matrix shown in Table 5 shows the AI system performance. The AI system accurately detected 257 of the 285 SFT patterns, which represented an overall accuracy of 90.18%. More precisely, it obtained a 92.73% accuracy in recognising 30s-CST patterns and an 86.67% accuracy in recognising 40m-FPWT patterns.

V. Conclusion

Human movement analysis is becoming a more popular area of research as wearable technology becomes more widely used in ambulatory settings. Wearable IMU sensors can gather data

on the wearers daily activities. However, the large number of data points recorded when monitoring over a long time period can make analysis quite cumbersome when compared to data recorded in a hospital environment. Movement data may contain feature rich information on the wearers physical health. Analysing and detecting specific activity patterns within sensor data may aid in enabling the provision of personalised rehabilitation programmes in the patient's home.

An ANN system trained with various clinical trial datasets for pattern recognition and pattern matching can recognize different SFT patterns from long-term data sets. This research utilized DL algorithms and an AI system to detect the 30s-CST and 40m-FPWT SFTS from data collected from participants using ViMove wearable sensors. Results showed a high level of SFT detection accuracy. The techniques used in this study can be used to automatically detect SFTs within long-term data to track patient activity and recovery at home. A point of interest is that some SFTs may be better characterized/recognized by implementing additional IMU sensors in the upper or lower limbs. For ambulatory monitoring, a minimal number of sensors located on the lower back proved to be sufficient to collect SFTs. In the future, this approach could be expanded by training the AI system to extract the Timed Up and Go (TUG) Test SFT pattern from ambulatory data. Furthermore, we could incorporate transfer learning, multi-instance learning, and novel advancements in deep learning techniques that combine ANNs with support vector machines (SVM), random forests, support vector regression (SVR), and regression trees to address more intricate movement pattern recognition problems.

The ability to automate the capture and isolation of 'snippets' of kinematic data on SFTs performed in the home will allow researchers to carry out more detailed analyses of these kinematics and monitor characteristic features to track the progress of a wide variety of disabling conditions including frailty, arthritis and neuromuscular disorders.

REFERENCES

[1] V. Strand and J. A. Singh, "Evaluation and Management of the Patient With Suspected Inflammatory Spine Disease," Mayo Clin. Proc., vol. 92, no. 4, pp. 555–564, 2017, doi: 10.1016/j.mayocp.2016.12.008.

[2] S. Skumlien, T. Hagelund, Ø. Bjørtuft, and M. S. Ryg, "A field test of functional status as performance of activities of daily living in COPD patients," Respir. Med., vol. 100, no. 2, pp. 316–323, 2006, doi: 10.1016/j.rmed.2005.04.022.

[3] N. Gebruers, C. Vanroy, S. Truijen, S. Engelborghs, and P. P. De Deyn, "Monitoring of Physical Activity After Stroke: A Systematic Review of Accelerometry-Based Measures," Arch. Phys. Med. Rehabil., vol. 91, no. 2, pp. 288–297, 2010, doi: 10.1016/j.apmr.2009.10.025.

[4] A. Salarian, F. B. Horak, C. Zampieri, P. Carlson-Kuhta, J. G. Nutt, and K. Aminian, "ITUG, a sensitive and reliable measure of mobility," IEEE Trans. Neural Syst. Rehabil. Eng., vol. 18, no. 3, pp. 303–310, 2010, doi: 10.1109/TNSRE.2010.2047606.

[5] J. Lee, D. Kim, H. Y. Ryoo, and B. S. Shin, "Sustainable wearables: Wearable technology for enhancing the quality of human life," Sustain., vol. 8, no. 5, 2016, doi: 10.3390/su8050466.

[6] H. Master et al., "A Narrative review on measurement properties of fixed-distance walk tests up to 40 meters for adults with knee osteoarthritis," J. Rheumatol., vol. 48, no. 5, pp. 638–647, 2021, doi: 10.3899/jrheum.200771.

[7] M. E. Mlinac and M. C. Feng, "Assessment of Activities of Daily Living, Self-Care, and Independence," Arch. Clin. Neuropsychol., vol. 31, no. 6, pp. 506–516, 2016, doi: 10.1093/arclin/acw049.

[8] Denise Myshko, "Wearables In clinical trials," BioPharm, vol. 10, no. 5, p. 12, 2019, doi: 10.1089/apc.1988.2.32.

[9] P. Schrangl, F. Reiterer, L. Heinemann, G. Freckmann, and L. del Re, "Limits to the evaluation of the accuracy of continuous glucose monitoring systems by clinical trials," Biosensors, vol. 8, no. 2, pp. 1–23, 2018, doi: 10.3390/bios8020050.

[10] P. H. S. Figueiredo et al., "The reliability and validity of the 30-seconds sit-to-stand test and its capacity for assessment of the functional status of hemodialysis patients," J. Bodyw. Mov. Ther., vol. 27, pp. 157–164, 2021, doi: 10.1016/j.jbmt.2021.02.020.

[11] P. Agarwala and S. H. Salzman, "Six-Minute Walk Test: Clinical Role, Technique, Coding, and Reimbursement," Chest, vol. 157, no. 3, pp. 603–611, 2020, doi: 10.1016/j.chest.2019.10.014.

[12] K. J. Fraser et al., "Wearable electrochemical sensors for monitoring performance athletes," Org. Semicond. Sensors Bioelectron. IV, vol. 8118, p. 81180C, 2011, doi: 10.1117/12.895109.

[13] I. Arun Faisal, T. Waluyo Purboyo, and A. Siswo Raharjo Ansori, "A Review of Accelerometer Sensor and Gyroscope Sensor in IMU Sensors on Motion Capture," J. Eng. Appl. Sci., vol. 15, no. 3, pp. 826–829, 2019, doi: 10.36478/jeasci.2020.826.829.

[14] B. Grimm and S. Bolink, "Evaluating physical function and activity in the elderly patient using wearable motion sensors," EFORT Open Rev., vol. 1, no. 5, pp. 112–120, 2016, doi: 10.1302/2058-5241.1.160022.

[15] L. Franco, R. Sengupta, L. Wade, and D. Cazzola, "A novel IMU-based clinical assessment protocol for Axial Spondyloarthritis: A protocol validation study," PeerJ, vol. 9, pp. 1–29, 2021, doi: 10.7717/peerj.10623.

[16] A. Choi, H. Jung, and J. H. Mun, "Single inertial sensor-based neural networks to estimate COM-COP inclination angle during walking," Sensors (Switzerland), vol. 19, no. 13, 2019, doi: 10.3390/s19132974.

[17] N. Diliberti, C. Peng, C. Kauffman, Y. Dong, and J. T. Hansberger, "Real-time gesture recognition using 3D sensory data and a light convolutional neural network," MM 2019 - Proc. 27th ACM Int. Conf. Multimed., pp. 401–410, 2019, doi: 10.1145/3343031.3350958.

[18] N. M. and D. H. * Gobinath Aroganam, "Consumer Sport Applications," 2019.

[19] C. Carmona-Pérez et al., "Concurrent validity and reliability of an inertial measurement unit for the assessment of craniocervical range of motion in subjects with cerebral palsy," Diagnostics, vol. 10, no. 2, 2020, doi: 10.3390/diagnostics10020080.

[20] V. Chandel, A. Sinharay, N. Ahmed, and A. Ghose, "Exploiting IMU sensors for IoT enabled health monitoring," IoTofHealth 2016 - Proc. 1st Work. IoT-Enabled Healthc. Wellness Technol. Syst. co-located with MobiSys 2016, pp. 21–22, 2016, doi: 10.1145/2933566.2933569.

[21] B. R. Greene, E. P. Doheny, K. McManus, and B. Caulfield, "Estimating balance, cognitive function, and falls risk using wearable sensors and the sit-to-stand test," Wearable Technol., vol. 3, 2022, doi: 10.1017/wtc.2022.6.

[22] A. Baştuğ and D. T. M. Slock, "Interference cancelling receivers with global MMSE-ZF structure and local MMSE operations," Conf. Rec. Asilomar Conf. Signals, Syst. Comput., vol. 1, no. 3, pp. 968–972, 2003, doi: 10.1109/acssc.2003.1292060.

[23] F. La Porta, S. Caselli, S. Susassi, P. Cavallini, A. Tennant, and M. Franceschini, "Is the berg balance scale an internally valid and reliable measure of balance across different etiologies in neurorehabilitation? A revisited rasch analysis study," Arch. Phys. Med. Rehabil., vol. 93, no. 7, pp. 1209–1216, 2012, doi: 10.1016/j.apmr.2012.02.020.

[24] J. Frost, "Spearman's Correlation Explained - Statistics By Jim." 2021. [Online]. Available: https://statisticsbyjim.com/basics/spearmans-correlation/

[25] U. Martinez-Hernandez and A. A. Dehghani-Sanij, "Probabilistic identification of sit-to-stand and stand-to-sit with a wearable

sensor," Pattern Recognit. Lett., vol. 118, pp. 32–41, 2019, doi: 10.1016/j.patrec.2018.03.020.

[26] D. J. Psaltos, F. Mamashli, T. Adamusiak, C. Demanuele, M. Santamaria, and M. D. Czech, "Wearable-Based Stair Climb Power Estimation and Activity Classification," Sensors, vol. 22, no. 17, 2022, doi: 10.3390/s22176600.

[27] A. Cobo et al., "Automatic and real-time computation of the 30-seconds chair-stand test without professional supervision for community-dwelling older adults," Sensors (Switzerland), vol. 20, no. 20, pp. 1–24, 2020, doi: 10.3390/s20205813.

[28] H. L. Mjøsund, E. Boyle, P. Kjaer, R. M. Mieritz, T. Skallgård, and P. Kent, "Clinically acceptable agreement between the ViMove wireless motion sensor system and the Vicon motion capture system when measuring lumbar region inclination motion in the sagittal and coronal planes," BMC Musculoskelet. Disord., vol. 18, no. 1, pp. 1–10, 2017, doi: 10.1186/s12891-017-1489-1.

[29] P. Kent, R. Laird, and T. Haines, "The effect of changing movement and posture using motion-sensor biofeedback, versus guidelines-based care, on the clinical outcomes of people with sub-acute or chronic low back pain-a multicentre, cluster-randomised, placebo-controlled, pilot trial," BMC Musculoskelet. Disord., vol. 16, no. 1, pp. 1–19, 2015, doi: 10.1186/s12891-015-0591-5.

[30] M. O'grady et al., "Measuring spinal mobility using an inertial measurement unit system: A reliability study in axial spondyloarthritis," Diagnostics, vol. 11, no. 3, pp. 1–17, 2021, doi: 10.3390/diagnostics11030490.

[31] "ViMove – dorsaVi US," 2022. https://www.dorsavi.com/vimove/ (accessed Oct. 14, 2022).

[32] V. Vijayan et al., "AI Techniques to Automatically Detect Standardized Functional Test Patterns from Wearable Sensor Data," 2022 33rd Irish Signals Syst. Conf. ISSC 2022, 2022, doi: 10.1109/ISSC55427.2022.9826154.

[33] C. J. Jones, R. E. Rikli, and W. C. Beam, "A 30-s chair-stand test as a measure of lower body strength in community-residing older adults," Res. Q. Exerc. Sport, vol. 70, no. 2, pp. 113–119, 1999, doi: 10.1080/02701367.1999.10608028.

[34] F. Dobson et al., "OARSI recommended performance-based tests to assess physical function in people diagnosed with hip or knee osteoarthritis," Osteoarthr. Cartil., vol. 21, no. 8, pp. 1042–1052, 2013, doi: 10.1016/j.joca.2013.05.002.

[35] R. P. Burn, "Quaternions and rotations," Groups, vol. 1, pp. 178–184, 2012, doi: 10.1017/cbo9781139163590.020.

[36] V. Vijayan, J. Connolly, J. Condell, P. Gardiner, and N. McKelvey, "Pattern matching techniques to automatically detect range of movement tests from wearable sensors," 2021 32nd Irish Signals Syst. Conf. ISSC 2021, pp. 1–6, 2021, doi: 10.1109/ISSC52156.2021.9467875.

[37] C. P. Robinson, B. Li, Q. Meng, and M. T. G. Pain, "Pattern classification of hand movements using time domain features of electromyography," ACM Int. Conf. Proceeding Ser., vol. Part F1291, 2017, doi: 10.1145/3077981.3078031.

[38] A. Neural and N. Models, "- :?he Analysis and Improvement of Artificial Neural Network Models," pp. 7–13, 1997.

[39] K. O. Shea and R. Nash, "An Introduction to Convolutional Neural Networks," pp. 1–11.

[40] J. Zupan, "Introduction to Artificial Neural Network (ANN) Methods : What They Are and How to Use Them Introduction to Artificial Neural Network (ANN) Methods : What They Are and How to Use Them *.," no. January 1994, 2014.

[41] P. Pandey, "Multi-Digit Number Classification using MNIST and ANN," vol. 9, no. 05, pp. 415–421, 2020.

[42] J. K. Basu, D. Bhattacharyya, and T. Kim, "Use of Artificial Neural Network in Pattern Recognition," no. May, 2020.

[43] R. Borràs, "Introduction to Deep Learning with TensoRflow and KeRas libraries with some examples in biomedical research at the Hospital Clínic of Barcelona," no. May, 2018.

[44] S. R. Dubey, S. K. Singh, and B. B. Chaudhuri, "Activation Functions in Deep Learning: A Comprehensive Survey and Benchmark".

[45] T. Szanda and T. Wroclaw, "Review and Comparison of Commonly Used Activation Functions for Deep Neural Networks," 2018.

[46] F. Manessi and A. Rozza, "Learning Combinations of Activation Functions," Proc. - Int. Conf. Pattern Recognit., vol. 2018-Augus, pp. 61–66, 2018, doi: 10.1109/ICPR.2018.8545362.